Scaling relations for seismic cycles on mid-ocean ridge transform faults

Margaret S. Boettcher[1] and Jeffrey J. McGuire[2]

[1]   Mid-ocean ridge transform faults (RTFs) have thermal structures that vary systematically with tectonic parameters, resulting in predictable seismic characteristics and clear seismic cycles. We develop a scaling relation for repeat time, t_R, of the largest expected earthquake, M_C: $t_R = \mu^{-1} \Delta\sigma^{2/3} C_{Mc} A_T^{1/4} V^{-1}$, where μ is the shear modulus, $\Delta\sigma$ is the stress drop, C_{Mc} is a constant, A_T is the area above $600°C$, and V is the slip rate. We identify repeating M_C earthquakes by measuring differential arrival times of first orbit Rayleigh waves to determine centroid offsets between pairs of events. Comparing our observations of t_R ($5–14$ years for earthquakes on Gofar and Blanco RTFs) with predictions from our scaling relation, we can constrain RTF stress drops. Specific tests of this scaling relation are proposed for earthquakes on Blanco, Gofar, Discovery, and Clipperton RTFs, which are all expected to have large ruptures in the next few years. **Citation:** Boettcher, M. S., and J. J. McGuire (2009), Scaling relations for seismic cycles on mid-ocean ridge transform faults, *Geophys. Res. Lett.*, *36*, L21301, doi:10.1029/ 2009GL040115.

1.   Introduction

[2]   By contrast to slip on continental strike-slip faults, slip on mid-ocean ridge transform faults (RTFs) is largely aseismic [e.g., *Brune*, 1968; *Bird et al.*, 2002; *Boettcher and Jordan*, 2004; *Frohlich and Wetzel*, 2007] and magnitudes of the largest earthquakes are small ($6 \leq M_W \leq 7.1$) compared to the large RTF areas [e.g., *Bird et al.*, 2002; *Boettcher and Jordan*, 2004]. Seismicity on RTFs is known to follow a tapered frequency-moment distribution [e.g., *Kagan and Jackson*, 2000],

$$N(M) = N_0 \left(\frac{M_0}{M}\right)^{\beta} \exp\left(\frac{M_0 - M}{M_C}\right), \quad (1)$$

where N_0 is the cumulative number of events above the completeness threshold moment M_0 and β is the slope of the distribution below the exponential roll off at M_C, which is the seismic moment of the largest expected earthquake.

[3]   Thermal processes appear to have a strong control on RTF seismicity. Earthquake focal depths [e.g., *Abercrombie and Ekström*, 2001; *Braunmiller and Nábělek*, 2008] and laboratory friction experiments [*Boettcher et al.*, 2007] indicate that base of the seismogenic zone on RTFs is bounded by the $600°C$ isotherm. *Boettcher and Jordan*

[2004] found that RTF seismic parameters, including M_C, scale with the area of the seismogenic zone A_T, which they approximated using the half-space cooling model as $A_T = C_T L^{3/2} V^{-1/2}$, where the constant C_T depends on the isotherm chosen as the base of the seismogenic zone. For $600°C$, C_T is 4.1×10^3 km/yr$^{1/2}$. Improved thermal models that incorporate brittle behavior and temperature-dependent rheology [*Behn et al.*, 2007], as well as frictional heating and hydrothermal cooling [*Roland et al.*, 2007], predict altered isotherm shapes, yet the magnitude of A_T remains roughly unchanged.

[4]   Fast slipping RTFs with small A_T show clear seismic cycles, where M_C earthquakes reoccur when $\sim$70 cm of plate motion accumulates after the previous large earthquake [*McGuire*, 2008]. These observations suggest that the fault patch ruptured during an M_C earthquake is fully coupled, i.e., only slips during seismic events. Furthermore, *McGuire*'s [2008] results imply that slip in the rupture zone of a M_C earthquake is "single-mode", where the fault patch slips only seismically, in contrast to a "multi-mode" fault patch, where slip may be both seismic and aseismic [*Boettcher and Jordan*, 2004]. Here we develop a scaling relation for repeat times of M_C earthquakes and use it to explore the suggestion of full coupling on M_C patches.

2.   Verification of Scaling Relations With Recent RTF Seismicity

[5]   *Boettcher and Jordan* [2004, hereinafter referred to as BJ], showed that the tectonic parameters (lengths L and slip rates V) can be used to predict the seismic parameters of RTFs, including the moment of the largest expected event, M_C, and the total moment release, $\sum M$. Here we test the validity of these scaling relations, which were derived using seismicity from 1964–2001, by assessing their ability to predict seismicity from January 2002 through June 2009. Strike-slip earthquakes that occurred on the 65 largest RTFs were obtained from the Global CMT Project (G. Ekström et al., http://www.globalcmt.org/, 2009) using BJ's selection criteria [see *Boettcher and Jordan*, 2004, section 4.1 and Table B1]. The global frequency-moment distribution from these earthquakes (circles in Figure 1) can be compared with predicted distributions (curves in Figure 1) that were synthesized from equation (1) using $M_0 = 3.2 \times 10^{17}$ Nm, $\beta = 2/3$, and RTF lengths and slip rates. M_C and N_0 were calculated using the assumptions described in the following paragraphs.

[6]   To calculate M_C, we follow BJ and assume that slip, D_C, during an M_C earthquake scales as the square root of the rupture area, A_C, as $D_C = \Delta\sigma\mu^{-1}A_C^{1/2}$, and the static stress drop, $\Delta\sigma$, is assumed to be independent of earthquake size. From the definition of seismic moment, $M_C = \mu A_C D_C$, and our expression for D_C, we find $M_C = \Delta\sigma A_C^{3/2}$. The next step in

---
[1]Department of Earth Sciences, University of New Hampshire, Durham, New Hampshire, USA.
[2]Department of Marine Geology and Geophysics, Woods Hole Oceanographic Institution, Woods Hole, Massachusetts, USA.
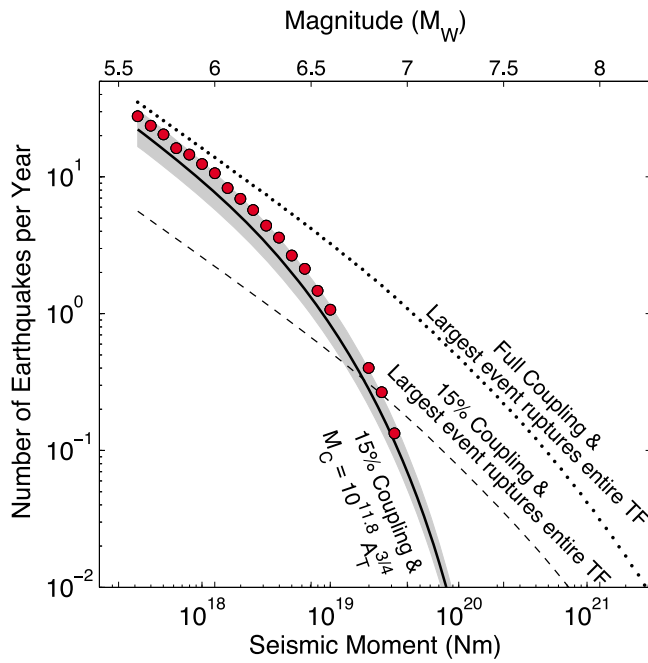
Figure 1. The cumulative frequency-moment distribution of seismicity from the Global CMT catalog, January 2002 to June 2009 (solid circles), fits well with *Boettcher and Jordan's* [2004] scaling relations derived from global seismic catalogs (CMT and ISC) with data from 1964 to 2001 (solid curve shows best fit parameters, and gray shading shows the 95% confidence limits). Each of the model curves is constructed from a frequency-moment relation (equation (1)), RTF lengths and slip rates, a chosen coupling coefficient, and a scaling relation for the largest event as described in the text.

determining M_C is to assume a scaling relation between A_C and the total fault area, A_T. The simplest assumption is that the largest earthquake ruptures the entire fault, $A_C = A_T$, which yields $M_C^{A_T} = \Delta\sigma A_T^{3/2}$. Another possibility is to assume $A_C \propto A_T^{1/2}$, as observed by BJ, which yields $M_C^{obs} = C_{Mc} A_T^{3/4}$. BJ's observed scaling accounts for both the expected positive correlation between M_C and L [see *Boettcher and Jordan*, 2004, Appendix C] as well as the negative correlation between M_C and V that is found in many studies of RTFs [*Bird et al.*, 2002; *Langenhorst and Okal*, 2002; *Boettcher and Jordan*, 2004].

[7] To calculate N_0 we use BJ's observation of a constant seismic coupling coefficient χ, which is the ratio between the total seismic slip on an RTF, $D_{Seismic} = \sum M/(\mu A_T)$, and the plate tectonic slip during the same time period, $D_{Tectonic} = V t_{cat}$. BJ show that the total seismic moment derived from equation (1) is $\sum M \approx N_0 M_0^\beta M_C^{1-\beta} \Gamma(1-\beta)$ where the gamma function is $\Gamma(1/3) = 2.678...$. The shear modulus μ is taken to be 44.1 GPa, which is between values for gabbro and peridotite and is the lower crustal value from the Preliminary Reference Earth Model (PREM) [*Dziewonski and Anderson*, 1981], which was used to determine seismic moment for RTF earthquakes in the Global CMT catalog. N_0 can then be determined for any catalog interval, t_{cat}, from $\chi = D_{Seismic}/D_{Tectonic}$ as $N_0 = \chi \mu t_{cat} M_0^{-2/3} M_C^{-1/3} A_T \Gamma(1/3)^{-1}$.

[8] Frequency-moment distributions were synthesized individually for each of the 65 RTFs and then summed to

produce the curves in Figure 1. We assumed either full coupling ($\chi = 1$, dotted curve) or BJ's observed coupling coefficient ($\chi = 0.15^{+0.03}_{-0.02}$, dashed and solid curves). Similarly, for each RTF we assumed that either the largest earthquake ruptured the entire fault ($M_C = M_C^{A_T}$) with a stress drop of $\Delta\sigma = 3$ MPa (dotted and dashed curves), or we used BJ's observed scaling ($M_C = M_C^{obs}$) with their observed coefficient ($C_{Mc} = \exp(11.80^{+0.2}_{-0.2})$, solid curve). The gray shading in Figure 1 incorporates the uncertainty in the observed values of both χ and C_{Mc}. The recent RTF earthquakes follow BJ's scaling relations, supporting their assertion that the rupture area of M_C earthquakes does not scale linearly with the total fault area. While the seismicity rate between 2002–2009 appears to be slightly higher than predicted by BJ's scaling relations (black curve in Figure 1), the difference is indistinguishable at the 95% confidence level. Using the same technique to calculate the maximum likelihood parameters from the 2002–2009 data, we obtain the values $\chi = 0.20^{+0.05}_{-0.03}$ and $C_{Mc} = \exp(11.7^{+0.3}_{-0.3})$, which overlap with those from BJ.

3. Scaling Relation for Repeat Time

[9] After verifying that BJ's scaling relations successfully predict future distributions of RTF seismicity, we now extend them to include repeat time t_R for M_C earthquakes. To calculate t_R we make the assumption that each fault patch ruptured by an M_C earthquake is fully coupled. With this assumption, the repeat time is the ratio of the earthquake slip to the plate tectonic slip rate, $t_R = D_C/V$. Our next assumption is that slip scales with square root of rupture area, $D_C = \Delta\sigma\mu^{-1}A_C^{1/2}$. Solving the definition of seismic moment for D_C yields $D_C = \mu^{-1}\Delta\sigma^{2/3}M_C^{1/3}$. Substituting this new expression for D_C into $t_R = D_C/V$ along with BJ's observed scaling $M_C^{obs} = C_{Mc}A_T^{3/4}$ (C_{Mc} is empirically fit in *Boettcher and Jordan*, 2004) gives

$$t_R = \frac{\Delta\sigma^{2/3}C_{Mc}^{1/3}A_T^{1/4}}{\mu V}, \qquad (2)$$

where t_R is directly proportional to the thermal scaling parameter, $A_T^{1/4}V^{-1}$. Equivalently, the repeat time can be written in terms of the directly observable plate tectonic parameters, L and V, as $t_R = \mu^{-1}\Delta\sigma^{2/3}C_{Mc}^{1/3}C_T^{1/4}L^{3/8}V^{-9/8}$. To explore whether our assumption of full seismic coupling on M_C fault patches is reasonable, we next compare observed repeat times with predicted values of t_R from equation (2).

4. Relocations of the Largest Expected Earthquakes on Selected RTFs

[10] While no two large earthquakes are identical, a logical criterion for defining repeating M_C earthquakes is that their rupture areas, A_C, have considerable overlap. Because rupture area for most RTF earthquakes cannot be determined directly from teleseismic data, we follow the approach of *McGuire* [2008] to determine the separation distances between the centroids of $M_W > 6$ earthquakes. To constrain the relative offset between event pairs we measure differential arrival times of 1st orbit Rayleigh waves by cross correlation in the frequency band 0.02–0.04 Hz. This
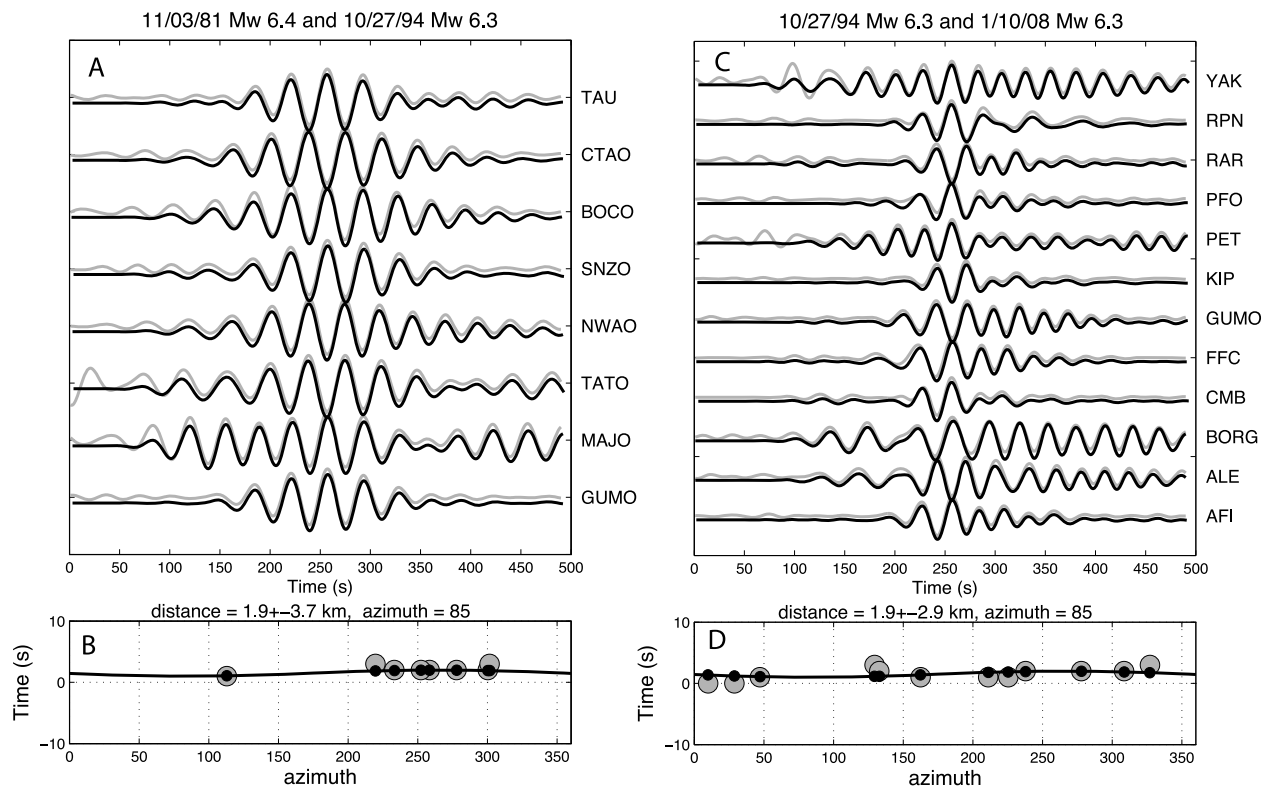
Figure 2. Relative relocations of the 1981, 1994, and 2008 Blanco Ridge earthquakes. (a) Rayleigh waveforms of the 1981 (gray) and 1994 (black) at GSN stations filtered between 0.02 and 0.04 Hz. (b) Differential arrival times (gray circles) and best fit estimates (black circles) for a 1.9 km offset at 85 degrees azimuth for the stations in Figure 2a. (c) Rayleigh waves of the 1994 (gray) and 2008 (black) earthquakes at GSN stations. (d) Differential arrival times (gray circles) and best fit estimates (black circles) for a 1.9 km offset at 85 degrees azimuth for the stations in Figure 2c. Figures 2b and 2d demonstrate that there is no resolvable difference in the centroid locations for the 1981 M_W 6.4, 1994 M_W 6.3, and 2008 M_W 6.3 earthquakes.

band is chosen for its high signal to noise ratio and because within it the R1 group velocity is fairly constant for young oceanic lithosphere [*Nishimura and Forsyth*, 1988], which allows arrival times to be interpreted in terms of source location differences rather than dispersion [*Forsyth et al.*, 2003]. The low-frequency band and small centroid separation distances result in cross-correlation coefficients that typically exceed 0.95 (Figure 2). Differential arrival times are measured from the peak of the cross-correlation functions, which are fit to a cosine function using an L1 norm to minimize the effect of occasional outliers. The azimuth and direction of the offset between two earthquakes are calculated using the scale and phase parameters of the cosine function along with the group velocity of the R1 waves in the source region (~3.7 km/s). The only significant difference from the approach of *McGuire* [2008] is that here we first deconvolve the instrument response to allow cross-correlations between recordings from the 1980s with those made in the 1990s and 2000s on upgraded Global Seismic Network (GSN) stations.

[11] We have determined relative locations for M_W 6.0–6.4 earthquakes that occurred in 1981, 1985, 1994, 2000, and 2008 on the Blanco Ridge segment of the Blanco RTF (Table 1 and Figures 2 and S2).[1] The 1981, 1994, and 2008

M_W 6.3–6.4 earthquakes have indistinguishable centroids (Figure 2 and Table 1), as indicated by separation offsets of less than 10 km, where rupture lengths of M_W 6.0–6.4 RTF earthquakes are expected to be 20–40 km based on aftershock locations [*Dziak et al.*, 2000; *McGuire*, 2008]. Similarly, the 1985 and 2000 M_W 6.0–6.4 earthquakes have indistinguishable centroids (Table 1) that are located approximately 25 km east of the 1981–1994–2008 centroids. Our location for the 1994 event agrees with *Dziak et al.*'s [2000] aftershock locations and with *Braunmiller and Nábĕlek* [2008], who showed that rupture propagated towards the west. Thus, the Blanco Ridge segment of the Blanco RTF appears to have two distinct segments, one centered at ~128.0°W and one centered at ~127.7°W that fail independently, but with similar recurrence intervals of $t_R \approx 13.5$ years.

[12] We have also updated the catalog of repeating large ruptures on the Discovery and Gofar RTFs from *McGuire* [2008] to include the 2008 M_W 6.0 earthquake on the G3 segment of Gofar and the 2009 M_W 5.5 earthquake on the D1 segment of Discovery (Table 1 and Figure S1). Both of these events have indistinguishable centroids from previous similar-sized earthquakes. The 2008 Gofar event is particularly interesting in that we have now recorded three complete cycles (four earthquakes: 1992, 1997, 2003, 2008), with indistinguishable centroids, on a single asper-

Table 1. Relative Relocation of M_C Earthquakes

RTF Segment[a]	Event 1			Event 2			Separation	Azimuth	M_0 Ratio	Δt (yr)
	Date	Time	M_W	Date	Time	M_W				
BR-E	03/13/85	19:35:02	6.4	01/20/00	09:41:53	6.0	3.7 ± 5.5	85	3.7	14.9
BR-W	10/27/94	17:46:07	6.3	01/10/08	01:37:24	6.3	1.9 ± 2.9	85	1.1	13.2
BR-W	11/03/81	13:47:37	6.4	10/27/94	17:46:07	6.3	1.9 ± 4.5	85	1.5	13
BR	10/27/94	17:46:07	6.3	01/20/00	09:41:54	6.0	25 ± 3.8	100	-	-
BR	11/03/81	13:47:37	6.4	03/13/85	07:35:02	6.4	14 ± 3.1	100	-	-
G3	09/06/03	02:08:19	6.0	09/18/08	01:41:07	6.0	3.7 ± 3.7	100	1.1	5
D1	07/30/01	04:34:51	5.6	05/24/09	00:58:09	5.6	1.9 ± 3.3	30	1.1	7.8

[a]BR-E and BR-W, east and west rupture zones on the Blanco Ridge segment of Blanco RTF; G3, westernmost segment of Gofar RTF; and D1, easternmost segment of Discovery RTF. The data are shown in Figure 2 and in Figures S1 and S2.

ity (M_C fault patch). Each cycle lasted approximately 5 years.

5. Discussion

[13] With the scaling relation for t_R given in equation (2) and our observations of relatively stable seismic cycles on a few RTFs, we can now compare predicted and observed values of repeat times for M_C earthquakes. The comparison in Figure 3 between the observed repeat times for M_C earthquakes on six segments of the Blanco, Gofar, and Discovery RTFs (Table 2) and repeat times predicted from the scaling relation for t_R (equation (2)) indicate that RTF stress drops are on the order of $3-10$ MPa, at least for M_C earthquakes on medium to fast slipping RTFs. While our inferred stress drops are approximately the same as a recent global average over all tectonic environments [*Allmann and Shearer*, 2009], our stress drop estimates are lower than might be expected based on high-velocity friction experiments on peridotite that show almost complete dynamic stress drops [*Del Gaudio et al.*, 2009]. It is important to note that the scaling relation for t_R is dependent on shear modulus, which for some RTFs with small A_T may be lower
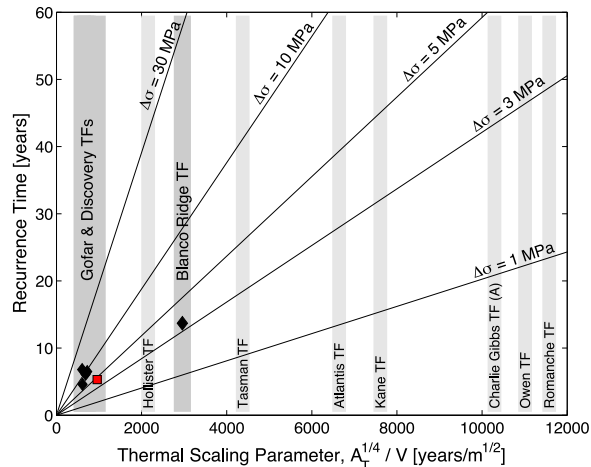

Figure 3. Recurrence times for a range of stress drops versus fault thermal scaling parameter, $A_T^{1/4}/V$, for selected RTFs. Black diamonds show observed recurrence times for repeating earthquakes on Gofar, Discovery, and Blanco RTFs (Table 2) and red square shows the recurrence time for the Western Gofar segment, for which three complete seismic cycles have been recorded. Stress drops of about $3-10$ MPa may be common for RTF earthquakes.

than the PREM value for lower crust used here. The lower values used in other RTF studies, $27 \le \mu \le 35$ GPa [e.g., *Gregg et al.*, 2006; *Braunmiller and Nábělek*, 2008], would only decrease our stress drop values by at most a factor of 1.6 ($\Delta\sigma = 2-6$ MPa). A test of our proposed scaling relation for t_R will be whether stress drops on Blanco, Gofar, and Discovery RTFs are in fact $2-10$ MPa. It will soon be possible to accurately estimate rupture area, and hence stress drop, for M_C earthquakes from ocean bottom seismic deployments.

[14] Clipperton RTF on the East Pacific Rise (EPR) stands out from most other RTFs in its ability to generate large earthquakes relative to it's thermal area, and therefore we examine whether it will constitute a contradiction to our scaling relation for repeat time. The largest earthquakes on Clipperton (M_W 6.6) are significantly larger than expected (M_W 6.1) based on BJ's scaling relations and χ is more than three times the median RTF value. These differences may be due to the transpressional nature of Clipperton, caused by recent changes in the Pacific Plate's direction of motion, which likely results in a higher normal stress [*Pockalny et al.*, 1997]. The increased normal stress might suggest that stress drops on Clipperton would also be higher.

[15] Two $M_W > 5.7$ earthquakes have been recorded on Clipperton since the start of the Global CMT catalog in 1976, both were M_W 6.6: Dec. 25, 1978 at 10.41°N, 103.80°W and Dec. 1, 1995 at 10.38°N, 103.88°W. While data from 1978 cannot be easily relocated using the technique described in section 3, given the event sizes and locations, it is likely that the M_W 6.6 events were repeating M_C earthquakes. From Clipperton's length (90 km), slip rate (105 mm/yr), and the observed recurrence interval (17 years), we obtain a stress drop from our scaling relation (2) of $\Delta\sigma = 17$ MPa. This value is about a factor of two higher than our previously determined stress drops. Clipperton will form an interesting test case as equation (2) predicts that a M_W 6.6 earthquake should repeat in the next few years with a high-stress drop. Additionally, equation (2) predicts a

Table 2. Mean Seismic Cycle Parameters for RTF Segments

RTF Segment[a]	t_R (years)	L (km)	M_C Magnitude
BR	13.7	150	6.4
G1	6.5	45	6.1
G2	4.6	29	5.8
G3	5.3	95	6.2
D1	6.8	28	5.6
D2	6.1	39	6.0

[a]BR, Blanco Ridge segment of Blanco RTF; G1, G2, and G3, segments of Gofar RTF; and D1 and D2, segments of Discovery RTF.

rupture length of $17-26$ km, assuming the rupture width is $4-6$ km and $\Delta\sigma = 17$ MPa. If this repeat event does not occur, or if it occurs with a lower stress drop, it would be an argument against full coupling for the M_C patches and instead it would be an argument in favor of the multimode hypothesis.

6. Conclusions

[16] We have attempted to develop a test to elucidate why the rupture areas of the largest earthquakes on RTFs do not scale directly with the area above the 600°C isotherm. Both the Blanco and Gofar RTFs appear to be comprised of multiple patches on a single fault segment that repeatedly fail in M_C sized earthquakes. Moreover, based on BJ's global compilation, a complete rupture of an entire A_T sized patch on an RTF has not happened during the historical record. If the stress drops of the Gofar and Blanco earthquakes agree with our estimate of $3-10$ MPa from Figure 3, then an A_C sized patch is likely to be a fully-coupled, single-mode fault segment. The difference between A_T and A_C would have to be explained by along-strike variations in frictional stability. The primary question would then become: why is there a barrier to rupture propagation between the two M_C patches on the Blanco Ridge and Gofar G3 fault segments? Moreover, the global observed scaling relation $M_C^{obs} = C_{Mc}A_T^{3/4}$ would imply that whatever process creates these barriers to rupture propagation is systematically tied to fault thermal structure. In contrast, if the stress-drops do not match the predictions for the Blanco, Gofar, and Clipperton faults, that will imply a multimode behavior for the M_C sized fault patches. The multimode behavior would then require a dynamic effect to limit the size of an individual rupture from reaching the whole fault.

References

Abercrombie, R., and G. Ekström (2001), Earthquake slip on oceanic transform faults, *Nature*, *410*, 74–77, doi:10.1038/35065064.

Allmann, B. P., and P. M. Shearer (2009), Global variations of stress drop for moderate to large earthquakes, *J. Geophys. Res.*, *114*, B01310, doi:10.1029/2008JB005821.

Behn, M. D., et al. (2007), On the thermal structure of oceanic transform faults, *Geology*, *35*, 307–310, doi:10.1130/G23112A.1.

Bird, P., Y. Y. Kagan, and D. D. Jackson (2002), Plate tectonics and earthquake potential of spreading ridges and oceanic transform faults, in *Plate Boundary Zones, Geodyn. Monogr. Ser.*, vol. 30, edited by S. Stein and J. T. Freymueller, pp. 203–218AGU, Washington, D. C.

Boettcher, M. S., and T. H. Jordan (2004), Earthquake scaling relations for mid-ocean ridge transform faults, *J. Geophys. Res.*, *109*, B12302, doi:10.1029/2004JB003110.

Boettcher, M. S., G. Hirth, and B. Evans (2007), Olivine friction at the base of oceanic seismogenic zones, *J. Geophys. Res.*, *112*, B01205, doi:10.1029/2006JB004301.

Braunmiller, J., and J. Nábělek (2008), Segmentation of the Blanco Transform Fault Zone from earthquake analysis: Complex tectonics of an oceanic transform fault, *J. Geophys. Res.*, *113*, B07108, doi:10.1029/2007JB005213.

Brune, J. N. (1968), Seismic moment, seismicity, and rate of slip along major fault zones, *J. Geophys. Res.*, *73*, 777–784, doi:10.1029/JB073i002p00777.

Del Gaudio, P., G. Di Toro, R. Han, T. Hirose, S. Nielsen, T. Shimamoto, and A. Cavallo (2009), Frictional melting of peridotite and seismic slip, *J. Geophys. Res.*, *114*, B06306, doi:10.1029/2008JB005990.

Dziak, R. P., et al. (2000), Recent tectonics of the Blanco Ridge, eastern Blanco transform fault zone, *Mar. Geophys. Res.*, *21*, 423–450, doi:10.1023/A:1026545910893.

Dziewonski, A. M., and D. L. Anderson (1981), Preliminary reference Earth model, *Phys. Earth Planet. Inter.*, *25*, 297–356, doi:10.1016/0031-9201(81)90046-7.

Forsyth, D. W., Y. Yang, M.-D. Mangriotis, and Y. Shen (2003), Coupled seismic slip on adjacent oceanic transform faults, *Geophys. Res. Lett.*, *30*(12), 1618, doi:10.1029/2002GL016454.

Frohlich, C., and L. R. Wetzel (2007), Comparison of seismic moment release rates along different types of plate boundaries, *Geophys. J. Int.*, *171*, 909–920, doi:10.1111/j.1365-1246X.2007.03550.x.

Gregg, P. M., et al. (2006), Segmentation of transform systems on the East Pacific Rise: Implications for earthquake processes at fast-slipping oceanic transform faults, *Geology*, *34*, 289–292, doi:10.1130/G22212.22211.

Kagan, Y. Y., and D. D. Jackson (2000), Probabilistic forecasting of earthquakes, *Geophys. J. Int.*, *143*, 438–453, doi:10.1046/j.1365-246X.2000.01267.x.

Langenhorst, A. R., and E. A. Okal (2002), Correlation of beta-value with spreading rate for strike-slip earthquakes of the mid-oceanic ridge system, in *Plate Boundary Zones, Geodyn. Monogr. Ser.*, vol. 30, edited by S. Stein and J. T. Freymueller, pp. 191–202, AGU, Washington, D. C.

McGuire, J. J. (2008), Seismic cycles and earthquake predictability on East Pacific Rise transform faults, *Bull. Seismol. Soc. Am.*, *98*, 1067–1084, doi:1010.1785/0120070154.

Nishimura, C., and D. W. Forsyth (1988), Rayleigh wave phase velocities in the Pacific with implications for azimuthal anisotropy and lateral heterogeneities, *Geophys. J. R. Astron. Soc.*, *94*, 479–501.

Pockalny, R. A., P. J. Fox, D. J. Fornari, K. C. Macdonald, and M. R. Perfit (1997), Tectonic reconstruction of the Clipperton and Siqueiros Fracture Zones: Evidence and consequences of plate motion change for the last 3 Myr, *J. Geophys. Res.*, *102*, 3167–3181, doi:10.1029/96JB03391.

Roland, E. C., et al. (2007), Thermal-mechanical behavior of oceanic transform faults: Implications for hydration of the upper oceanic mantle, *Eos Trans. AGU*, *88*(52), Fall Meet. Suppl., , Abstract T32B-06.

―――――――――――

M. S. Boettcher, Department of Earth Sciences, University of New Hampshire, Durham, NH 03824, USA. (margaret.boettcher@unh.edu)

J. J. McGuire, Department of Marine Geology and Geophysics, Woods Hole Oceanographic Institution, Woods Hole, MA 02543, USA.